Design and operation of the in-vessel Cryopump for the new upper divertor in ASDEX Upgrade

G. Schall, N. Berger, D. Bösser, A. Herrmann, V. Rohde, M. Sochor, M. Weißgerber and the ASDEX Upgrade team

Max-Planck-Institut für Plasmaphysik, D-85748 Garching, Germany

To study alternative divertor configurations in the ASDEX Upgrade (AUG) tokamak a new upper divertor, Div-IIo, with two in-vessel coils and a cryopump (CP) will be installed in 2022. For efficient density control in the new divertor configuration during plasma discharges, the CP has to guarantee an effective pumping speed for deuterium (D_2) of at least S_{eff} = 15 m^3/s. The CP will be installed behind the inner divertor with a toroidal pumping gap of width 30 mm between the inner and outer divertor plates. It consists of 7 modules with a major radius of R = 1.2 m and a total active length of 5.4 m.

To investigate reactor relevant D_2-He gas mixtures during upper single null discharges, the liquid helium cryo-panels are coated with activated charcoal as cryosorbent.

For quick regeneration of the charcoal from the accumulated gases, heating wires on the cryo-panels are installed.

To reduce the pumping speed during high density discharges, an in-vessel cryo valve between two modules is installed. The pumping speed can be reduced by 35 %.

The cryo-panels operate with saturated liquid helium (LHe) at a temperature of 4.4 K. The thermal radiation shield consisting of reflector and chevron-baffle operate with saturated liquid nitrogen (LN_2) at 80 K. To supply the new upper CP with LHe and LN_2 the existing LHe-LN_2-supply of the lower CP will be used. Therefore, an additional distributor box and a multi-channel transfer line to the upper CP have been installed in 2019.

Keywords: ASDEX Upgrade, Cryopump, Activated charcoal, Divertor, magnetic configurations

1. Introduction

The ASDEX Upgrade tokamak will be equipped with a new upper divertor with two internal coils and a cryopump to study alternative magnetic configurations aiming to distribute the exhausted power over a larger area and to assess the feasibility of divertor solutions for DEMO [1, 2].

The components of the new upper divertor are represented in Fig.1. Two 52 kA coils Do1 and Do2, each with four turns are integrated into the support structure behind the upper outer divertor [3].

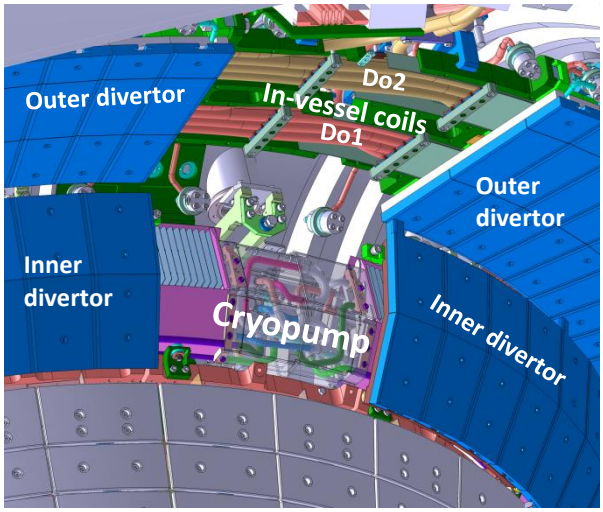

Fig.1: CAD view of the new upper divertor with the cryopump behind the inner divertor and the two internal coils Do1 and Do2 above the outer divertor.

The cryopump (CP) is designed for a deuterium pumping speed of 50 m^3/s. Owing to the 30 mm gap between the inner and outer divertor to the X-point region, an effective pumping speed of 21 m^3/s is calculated. To investigate high-density discharges, the pumping speed of the upper CP can be reduced by 35% with an in-vessel cryogenic valve analogous to the existing valve in the lower CP (65%).

The 4K cryosorption panels are coated with activated charcoal. This enables cryosorption of helium to investigate reactor-relevant D_2/He (5-10% He) exhaust gas mixtures. For desorption the accumulated gases, including H_2O by the activated charcoal, heating conductors are installed on the coated panels.

The entrance to the vertical diagnostic ports and the ability to mount the CP required a division into 7 toroidal CP modules, 5 short (≺35°) and 2 long (≺57°) units. To protect the pumping surface of the 4K cryopanels from radiation heat loads, the modules are surrounded by an 80K thermal radiation shield and a chevron baffle. Saturated liquid nitrogen (LN_2) is used as coolant for the 80K shield and chevron baffle. The 4K cryopanels will be supplied with saturated liquid helium (LHe).

The cryogenic cooling circuits of the CP modules are connected in series. To supply the upper CP with LHe and LN_2, the existing supply of the installed CP in the lower outer divertor can be used [4]. Only a distributor box and a LN_2 shielded multi-channel transfer line with 4 pipes to the upper CP are required.

The existing lower CP is a condensation pump w/o charcoal, consisting of 7 modules with 4K cryopanels made of 6 pieces of meandering shaped stainless steel tubes (11 x 0.5 mm). All cryogenic cooling circuits are routed in a series connection [5].

author's email: gerd.schall@ipp.mpg.de

2. Mechanical design and components of the cryopump

The design and components of the CP are shown in Fig. 2.

The cryogenic pipe connectors between two modules consist of corrugated pipes with copper-sealed flange connections and an 80K radiation shield casing. The flange connections allow disassembly of the CP modules for assembly work at the water flange connections of the heat shield between the CP and the vacuum vessel.

Torlon® 4203 (polyamide-imide) is used for the thermal and electrical insulation of the brackets on the 4K cryopanel and 80K shield reflector. To prevent high forces on the CP during plasma disruptions, the CP is electrically open in toroidal direction.

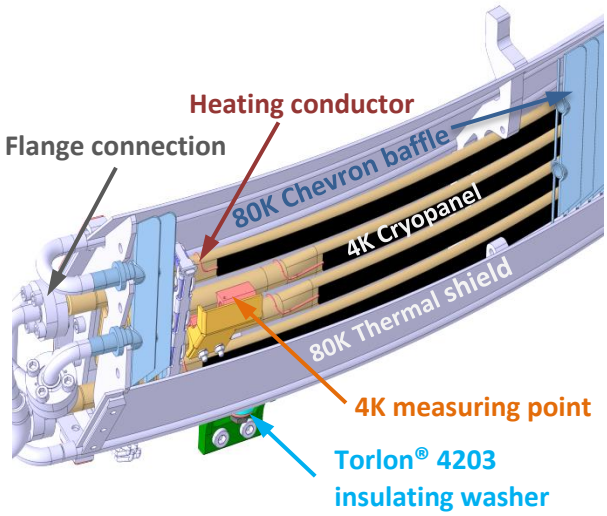

Fig. 2: CAD view of the main components of the cryopump.

2.1. 4K cryopanel

The 4K cryosorption panels consisting of 4 meandering oval formed stainless steel tubes with an outside-diameter 20 x 8 mm. As cryosorbent material to pump the gases, the oval tubes are coated on both 20 mm sides with activated charcoal which is bonded by ceramic glue to the sandblasted tube surface. The activated charcoal consists of coconut granules with a size of approximately 2 mm. The microporous charcoal has been extensively tested in the TITAN cryopanel test facility [6] and the TIMO test facility for the ITER cryopump at KIT [7] [8].

The total coated surface of the cryopanels is about 0.7 m^2 with a charcoal mass of m ≈ 350g. The adsorption capacity for He on the activated charcoal surface at 5K is about 300 Pa m^3 in the sorption equilibrium pressure at 2E-5 Pa (150 Pa m^3 @1E-5 Pa) [9].

To regenerate the CP, heating conductors are installed on both sides of the oval tubes. The cryopanels can be heated up to 470 K for fast desorption of water [10]. The required heating power is 100 W/m oval tube (400 W/module). 100K is sufficient to regenerate the CP from the gases He, D_2, H_2 [11].

A mass flow of 3 g/s LHe is required for a stable two-phase flow with saturated helium (1.2 bar, 4.4K). This guarantees a homogeneous distribution of the liquid/ vapor mixture and prevents the formation of larger gas bubbles and thus local heating of the 4K cryopanel.

The total pressure loss of the helium two-phase flow of the cryopump is 30 mbar @ 3 g/s (lower CP 100 mbar @ 4 g/s). The heat input into the 4K cryopanel between the plasma discharges (vacuum pressure 1e-5 Pa) is approximately 7 W. A heat input of approximately 45 W is calculated during the 10 s plasma discharges.

2.2. 80K thermal shield and chevron baffle

The thermal shields made of stainless steel plates are welded together with the series-connected LN_2 tubes. To minimize heat radiation losses, the thermal shields are electropolished.

The chevron baffle consists of lined up 90 ° angle plates made of stainless steel. To minimize the transmission radiation to the 4K cryopanel, the angle plates are chemically blackened. The heat input to the thermal shield by radiation (T_{vessel} = 293K) and heat conduction of the brackets is approximately 450W. A mass flow of 4 g/s LN_2 is sufficient for a homogeneous two-phase flow and cooling performance. The total pressure loss through the series-connected modules is 120 mbar (lower CP 300 mbar).

2.3. In-vessel cryogenic valve

In order to reduce the gas throughput during high-density discharges, the pumping speed of the CP can be reduced by 35% with an in-vessel cryogenic valve, see Fig. 3. The in-vessel valve is a combination of a 2-port/2-way valve and a 3-port/2-way valve, which is installed between two CP modules and enables the cooling of 4 modules with liquid helium.

For reduced operation, the two valve bellows are pressurized with 3.5 bar gaseous helium.

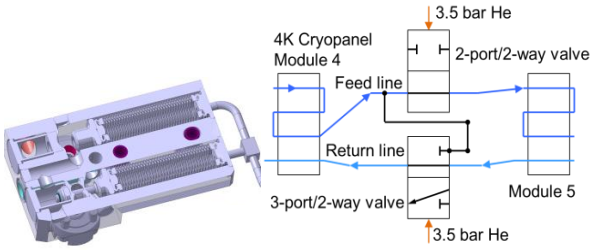

Fig.3: CAD cross section and flow chart of the in-vessel cryogenic valve.

3. Pumping speed

3.1. Pumping speed upper cryopump

The unsophisticated geometry of the cryopump, as shown in Figure 4, allows the analytical calculation of the pumping speed. The following Eq. (1) for calculating the pumping speed S includes the capture coefficient c which is the probability that a particle will pass the chevron baffle and be fixed by the cryopanel, the surface of the chevron baffle A_c (= 0.68 m^2) and the ideal pumping speed which is equal to the average

Maxwell gas velocity distribution in flow direction, which contains the universal gas constant R, ambient temperature T of the vacuum vessel and molecular mass M.

$$S = c \cdot A_c \cdot \sqrt{\frac{R \cdot T}{2 \cdot \pi \cdot M}} \qquad (1)$$

Owing to the gaps between the oval tubes of the 4K cryopanel, the particles which pass through the chevron baffle are reflected at the thermal shield. Thus, the particles can be impact on the entire oval tube surface. Eq. (2) is used to calculate the capture coefficient c of cryopump structures for double-sided pumping at the tubes of the 4K cryopanel [12]:

$$\frac{1}{c} = \frac{1}{\alpha \cdot (1-d) \cdot \left[1 + \frac{d}{d + \alpha \cdot (1-d)}\right]} + \frac{1}{w} - 1 \qquad (2)$$

where α is the sticking probability of the activated charcoal, the transmission probability w = 0.24 of the particles through the chevron baffle to the cryopanel, and the distance ratio d (=1/3) between the oval tubes. The term $\alpha \cdot (1-d) \cdot [1 + d/(d + \alpha \cdot (1-d))]$ is called the effective sticking coefficient α_e.

The sticking probabilities for fusion relevant gases at a charcoal temperature of 5K are according to [13] at initial zero gas load:

D_2 (α_{D2} = 0.9), H_2 (α_{H2} = 0.6), He (α_{He} = 0.35).

To calculate the effective pumping speed of the 4K cryopanel, the flow conductance C_{gap} (= pumping speed) through the gap opening (Fig.4: width w = 30 mm, length l = 35 mm) to the cryopanel is required. The equation for calculating the flow conductance through a gap opening is [14]:

$$C_{gap} = P \cdot A_{gap} \cdot \sqrt{\frac{R \cdot T}{2 \cdot \pi \cdot M}} \qquad (3)$$

with P being the transmission probability through the gap:

$$P = \frac{1 + ln(0.433 \cdot l/w + 1)}{l/w + 1} = 0.65 \qquad (4)$$

and the cross-section area with A_{gap} = 0.184 m^2.

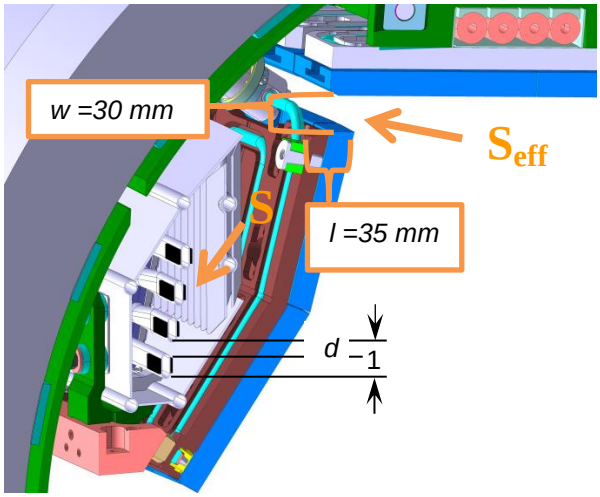

Fig. 4: Cross section of the cryopump and divertor plates with gap opening to the cryopump.

The effective pumping speed S_{eff} can be expressed by the reciprocal addition of the cryopanel pumping speed S and gap flow conductance C_{gap}.

$$\frac{1}{S_{eff}} = \frac{1}{S} + \frac{1}{C_{gap}} \qquad (5)$$

The results are summarized in table 1.

Table 1: Pumping speed of the 4K cryosorption panels.

	α @ 5K [13]	S (m^3/s)	S_{eff} (m^3/s)
D_2	0.9	48	21
H_2	0.6	61	28
He	0.35	36	18

3.2. Pumping speed lower cryopump

The calculated pumping speed for the lower condensation CP with the equations (1) (2) is in good agreement with the results of the measurements. Table 2 represents the calculated results for the gases D_2 and H_2.

Table 2: Calculated pumping speed of the lower condensation cryopump for the gases D_2 and H_2. Surface of the chevron baffle A_c = 2.45 m^2, distance ratio between the tubes d = 0.55, transmission probability w = 0.24.

	α @ 4.4K [12]	S (m^3/s)
D_2	0.85	158
H_2	0.85	223

The measured pumping speed S and S_{eff} are defined as the quotient of the gas throughput Q and measuring pressures p near the CP (S) and in the upper area of the vessel (S_{eff}). The pumping speeds are shown in Fig. 5.

$$S = \frac{Q}{p} \qquad (6)$$

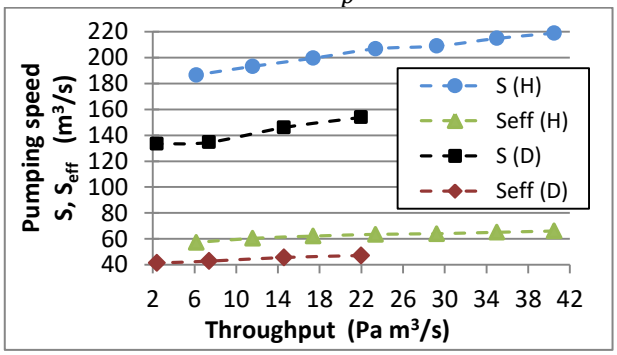

Fig. 5: Measured pumping speed S and effective pumping speed S_{eff} at the lower cryopump for the gases D_2 and H_2 at a temperature of the cryopanel of 4.4 K.

4. Operating modes of the upper and lower cryopump

4.1 Experimental operation:

At the beginning of the operation day, the cryopanels are cooled down to 4.4 K with saturated helium in approx. 45 min.

At the end of the day the cryopanels will be regenerated from the accumulated gases, mainly D_2 and H_2, by controlled warming up to 100 K using the installed heating conductors at the sorption panels of the upper CP. The condensation panels of the lower CP are regenerated by warming up to 20K via gas heat conduction at a vacuum pressure of 0.1 Pa.

The allowable accumulated hydrogen inventory for both cryopumps is limited to 19000 Pam^3. The released explosive gases are pumped out with an ATEX certified vacuum pump up to 500 Pa. Afterwards eleven turbomolecular pumps are switched on to guarantee the basic torus vacuum of 1e-5 Pa.

On weekends and before boronization of the vacuum vessel walls, the cryopumps are warmed up to an ambient temperature of 293K. The condensed water and hydrocarbons are released from the thermal shields, and can accumulate on the charcoal at the upper cryopanels. To regenerate the charcoal, the cryopanels are heated-up to 470 K.

The new upper cryopump can be used for upper single null D_2-He discharges. Owing to the limited He sorption capacity of the activated charcoal and to ensure a constant pumping speed, regular regeneration between the plasma discharges is necessary in this case.

4.2 Boronization:

At regular intervals the vessel walls are coated with a-BH layers for wall conditioning. A gas mixture of deuterated diborane (10%) and He (90%) is operated by glow discharge for several hours [15].

Experiments with activated charcoal and the diborane gas mixture have shown that the charcoal sorbs diborane, which causes problems due to toxicity and reduction of pumping capacity.

After laboratory investigations using propane as a proxy, final investigations were done at AUG, which is equipped to handle diborane, using the divertor manipulator. The tests were carried out with different charcoal temperatures (293K, 323K, 373K). The charcoal was exposed to the diborane gas mixture at a pressure of 1.5 Pa for 1 h. Subsequently, the gas was pumped out (< 1E-3 Pa). To release the accumulated diborane the charcoal was heated to 423K and continuously measured for diborane using a quadrupole mass spectrometer. The quadrupole was calibrated using a capacitance gauge for diborane. To get the total amount of released diborane, the background was subtracted and the calibrated masses 26 and 31 were integrated. The results are shown in Fig. 6.

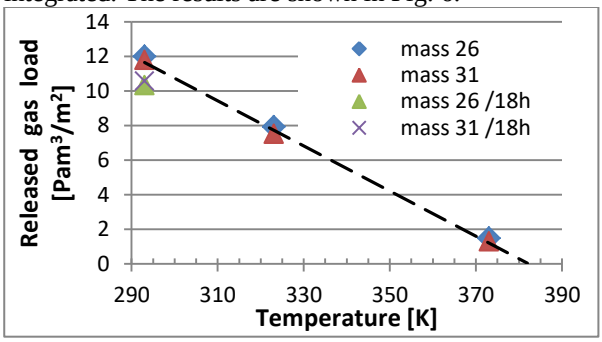

Fig. 6: Released gas load during heating the charcoal to 423K for exposed (diborane, 1 h @ 1.5 Pa) charcoal by temperatures 293K, 323K, 373K and 293K after 18 h pumping with a vacuum turbopump.

The amount for both masses agrees and the amount of captured diborane decreases with rising temperature. Additional the charcoal was loaded by 293 K and pumped overnight: only a small amount of diborane is released. It could be shown that pumping at room temperature is not sufficient to remove the diborane from the charcoal, but operation at 400 K will avoid sorption. Based on these results, the 4K cryopanel is heated to 400 K during boronization.

5. Summary

The cryopump is required for an effective density control in the divertor region to investigate advanced magnetic configurations with the new upper divertor Div-IIo. The cryopump is designed with 20 m^3/s (D_2) effective pumping speed in the private flux region. For high density discharges an in-vessel cryogenic valve can reduce the pumping speed to 13 m^3/s. Owing to the activated charcoal on the cryopanel, the cryopump can pump reactor-relevant D_2/He (5-10% He) exhaust gas mixtures.

6. Acknowledgements

This work has been carried out within the framework of the EUROfusion Consortium and has received funding from the Euratom research and training programme 2014-2018 and 2019-2020 under grant agreement No 633053. It also received extended funding within the Eurofusion PEX project. The views and opinions expressed herein do not necessarily reflect those of the European Commission.

References

[1] Lunt T., et al., Nucl. Mater. Energy 19 (2019) 107–112.
[2] Herrmann A., et al., Fusion Eng. Des. 123 (2017) 508–512.
[3] Herrmann A., et al., Fusion Eng. Des. 146 (2019) 920-923.
[4] Streibl B., et al., Operational behaviour of the ASDEX upgrade in-vessel cryo pump, Fusion Eng. Des. 56–7 (2001) 867–872.
[5] Streibl B., et al., Fusion technology, Proc. of the 19th Symposium on Fusion Technology, Lisbon, 1996, Elsevier, 1997, pp. 427-430.
[6] Day C., Colloids Surf. A Physicochem. Eng. Asp. 187-188 (2001) 187-206
[7] Haas H., Fusion Eng. Des. 69 (2003) 91-95.
[8] Day C., et al., Fusion Eng. Des. 86 (2011) 2188-2191.
[9] Day C., Basics and Applications of Cryopumps, (2007), pp. 244-245, ISBN 978-92-9083-294-2.
[10] Day Chr., Haas H., Fusion Eng. Des. 84 (2009) 665–668.
[11] Day C., Fusion Eng. Des. 81 (2006) 777–784.
[12] Haefer R.A., Kryo-Vakuumtechnik, Springer-Verlag Berlin Heidelberg GmbH 1981, ISBN 978-3-540-10167-3 / ISBN 978-3-642-49985-2 (eBook).
[13] Day C., et al. Vacuum 81 (2007) 738-747.
[14] Wutz M., Jousten K., Handbuch Vakuumtechnik, Springer Fachmedien Wiesbaden 2004, ISBN 978-3-322-96972-9 ISBN 978-3-322-96971-2 (eBook).
[15] Rohde V., et al., J. Nucl. Mater. 363-365 (2007) 1369.